http://ansinet.com/itj

ITJ

ISSN 1812-5638

INFORMATION TECHNOLOGY JOURNAL

ANSInet
Asian Network for Scientific Information
308 Lasani Town, Sargodha Road, Faisalabad - Pakistan

Information Technology Journal 8 (4): 486-494, 2009
ISSN 1812-5638

A Novel Method for Segmentation of the Cardiac MR Images using Generalized DDGVF Snake Models with Shape Priors

[1]Lixiong Liu, [1]Yuwei Wu and and [1,2]Yuanquan Wang
[1]Beijing Laboratory of Intelligent Information Technology, School of Computer Science and Technology, Beijing Institute of Technology, Beijing 100081, People's Republic of China
[2]Tianjin Key Lab of Intelligent Computing and Novel Software Technology, Tianjin University of Technology, Tianjin 300191, People's Republic of China

Abstract: In this study, a novel method is presented for segmentation of the endocardium and epicardium of the left ventricle in cardiac magnetic resonance images using snake models. We first generalize the DDGVF snake model by introducing two spatially varying weighting functions which characterize the boundary information; this generalized DDGVF snake can conquer the spurious edges raised by artifacts while maintaining the desirable properties of DDGVF of distinguishing the positive and negative boundaries. This is especially helpful for the tasks on hand because the endocardium and epicardium of the LV in MR images can be characterized as positive and negative boundaries. Observed that the left ventricle is roughly a circle, a shape constraint based on circle is introduced into the snake model. This new constraint can prevent the snake contour from being trapped and leaking out so as to maintain the global shape of the snake contour during evolution. In addition, fourth-order PDEs are employed for noise removal. We demonstrate the proposed approach on an *in vivo* dataset and compare the segmented contours with manual collections; the results show its effectiveness.

Key words: GVF snake, shape constraint, image segmentation, left ventricle, magnetic resonance imaging

INTRODUCTION

With excellent spatial and temporal resolution, cardiac Magnetic Resonance (MR) images can provide information about the cardiac anatomy and new insights on cardiac function in a noninvasive way. In order to make thorough use of the information derived from the images, the boundaries of the Left Ventricle (LV) should be extracted. Based on the segmentation results, some clinically established diagnosis indexes such as wall thickness, ejection fraction, etc., can be derived and an in-depth study of cardiac movement and strain can be launched, all these quantities can serve as objective reference for the prevention and treatment of cardiovascular disease.

In recent years, there has been a substantial amount of research on segmenting the LV from cardiac MR images. Efforts include morphologic segmentations (Fujino *et al*., 2001), fuzzy clustering (Lalande and Jaulent, 1996), model-based approaches (Bosch *et al*., 2001), active contour models (Kass *et al*., 1988; Xu and Prince, 1998; Osher and Sethiam, 1988) and etc. Among others, active contour models become extremely popular and dominated this field from its debut in 1988. For example, Ranganath *et al*. (1995) tracked the LV endocardium in image sequences based on snakes. Siddiqi *et al*. (1998) segmented the endocardium of the left and right ventricle simultaneously with a single initial curve by taking the advantages of level set. Makowski *et al*. (2002) made an improvement of the segmentation of complicated shapes such as papillary muscles in the LV by using the balloon snake models. Paragios (2003) integrated a statistical shape of the LV into the level set approach to segment the LV. Chen *et al*. (2004) proposed generalized fuzzy GVF for the segmentation and robust tracking of the LV in magnetic resonance images sequences. Under the level set framework, Pluempitiwiriyawej *et al*. (2005) presented a novel Stochastic Active Contour Scheme (STACS) for automatic image segmentation, which minimizes an energy functional that combines stochastic region-based and edge-based information with shape priors of the heart and local properties of the contour. Hautvast *et al*. (2006) developed a method that tries to maintain a constant contour environment by matching intensity profiles

Corresponding Author: Lixiong Liu, Beijing Laboratory of Intelligent Information Technology, School of Computer Science and Technology, Beijing Institute of Technology, Beijing 100081, People's Republic of China Tel: 86-10-68914849 Fax: 86-10-68914849

perpendicular to the contour. Wang and Jia (2006) proposed the energy constraints using shape similarities and a reformative edge map for GVF snakes to simultaneously extract the endocardium and epicardium of the LV. Folkesson *et al*. (2008) incorporated a statistical classifier trained using feature selection to segment the myocardium in Cardiac Late Gadolinium-Enhanced Magnetic Resonance Imaging (CE-MRI) data using coupled level set curves evolution.

However, accurate segmentation of the LV remains a challenging problem because of image inhomogeneity, especially artifacts resulted from swirling blood, papillary muscle and low contrast between the myocardium and neighbor organs such as the liver. The goal of this study is to present an effective and robust approach for LV segmentation from 2D MR images. The proposed method is based on GVF snake model, but thoroughly exploits the anatomy of the LV and the intensity properties of the MR images. The circle like anatomy of LV gives rise to a circle shape constraint being introduced into snake model; this global shape constraint can prevent the snake contour from being trapped and leaking out. By observing the intensity profile of the MR images, one can find that the endocardium of the LV is a positive boundary and the epicardium is a negative one. The DDGVF external force endows the snake models with the ability to discern positive and negative boundaries (Xu and Prince, 1998), but the DDGVF snake may be trapped into the spurious edges stemming from artifacts. Therefore, a generalized version of DDGVF is proposed by taking the edge information into account, this generalized DDGVF can overcome the spurious edges while maintaining other desirable properties of DDGVF such distinguishing the positive and negative boundaries. In a word, the snake model with generalized DDGVF external force and circle shape constraint can locate the endocardium and epicardium of the LV efficiently and accurately.

GENERALIZED DDGVF SNAKES

Brief review of GVF snake model: A snake is a curve $c(s) = (x(s), y(s)), s\in[0, 1]$, which moves through the spatial domain of an image to minimize the following energy functional:

$$E_{snake} = \int_0^1 E_{int}(c(s)) + E_{ext}(c(s))ds \quad (1)$$

where, E_{int} represents the internal energy of the snake contour, it reads:

$$E_{int} = \frac{1}{2}\left(\alpha|c_s(s)|^2 + \beta|c_{ss}(s)|^2\right) \quad (2)$$

where, α and β are two positive weights which control the elasticity and rigidity of the contour, respectively. c_s (s) and c_{ss} (s) denote respectively the first and the second derivatives of c(s) with respect to s. E_{ext} is the external energy, typically, the external energy for gray value image I is defined as:

$$E_{ext}(c(s)) = -|\nabla G_\sigma \otimes I|^2 \quad (3)$$

where, G_σ is the Gaussian kernel of standard deviation σ. Using the calculus of variations, a snake that minimizes E_{snake} must satisfy the Euler equation:

$$\alpha c_{ss}(s) - \beta c_{ssss}(s) - \nabla E_{ext} = 0 \quad (4)$$

This can be considered as a force balance equation:

$$F_{int} + F_{ext} = 0 \quad (5)$$

where, $F_{int} = \alpha c_{ss}(s) - \beta c_{ssss}(s)$ and $F_{ext} = \nabla E_{ext}$. The internal force F_{int} makes the snake contour to be smooth while the external force F_{ext} attracts the snake to the desired image features.

In a departure from this perspective, the gradient vector flow external force is introduced to replace $-\nabla E_{ext}$ with a new vector $v(x,y) = [u(x, y), v(x, y)]$ which is derived by minimizing the following function proposed by Xu and Prince (1998):

$$\varepsilon = \iint \mu|\nabla v|^2 + |\nabla f|^2|v - \nabla f|^2 dxdy \quad (6)$$

where, f is the edge map of an image, μ is a positive weight. Using the calculus of variation, the Euler equations seeking the minimum of ε read:

$$\mu\nabla^2 v - (v - \nabla f)(f_x^2 + f_y^2) = 0 \quad (7)$$

where, ∇^2 is the Laplacian operator. The snake model with v as external force is called GVF snake.

Generalized DDGVF snake models: Since the external energy, or external force, plays a leading role in driving the snake contour to approach objects, exploring effective external force is of paramount significance. Although GVF snakes define external energy by diffusing a certain gradient vector field, but the gradient vector field stems from the gradient magnitude of the image, which is a conventional step edge detector. As pointed out by Cheng and Say Wei (2006), the magnitude operator discards the signs of gradient, the snake is unable to

distinguish between positive and negative step edge. This associated problem handicaps the behavior of GVF snake. To deal with this problem, Cheng and Foo proposed the DDGVF to distinguish between positive boundary and negative boundary. Under their framework, a boundary is defined to be positive if there are positive step edges along its outward normal, i.e., the intensity gradients along the boundary are pointing inward. Contrarily, a boundary is negative if there are negative step edges along its outward normal. Here, we generalize the DDGVF by incorporating two spatially varying weighting functions which characterize the boundary information and refer to it as generalized DDGVF, GDDGVF in short. This improves active contour to conquer spurious weak edges while maintaining other desirable properties of DDGVF, such as an extended capture range and ability to distinguish positive and negative boundaries.

The GDDGVF field has four components: $v_{GDDGVF} = [u^+(x, y), u^- (x, y), v^+(x, y), v^-(x, y)]$ for four directions. These components are derived by solving the following diffusion equations:

$$\begin{cases} u_t^+ = p\cdot\nabla^2 u^+ - q\cdot f_x^+\left(u^+ - u_0^+\right), & u_0^+ = \dfrac{\partial f_x^+}{\partial x} \\ u_t^- = p\cdot\nabla^2 u^- - q\cdot f_x^-\left(u^- - u_0^-\right), & u_0^- = \dfrac{\partial f_x^-}{\partial x} \\ v_t^+ = p\cdot\nabla^2 v^+ - q\cdot f_y^+\left(v^+ - v_0^+\right), & v_0^+ = \dfrac{\partial f_y^+}{\partial y} \\ v_t^- = p\cdot\nabla^2 v^- - q\cdot f_y^-\left(v^- - v_0^-\right), & v_0^- = \dfrac{\partial f_y^-}{\partial y} \end{cases} \quad (8)$$

where, $p = \exp(-|\nabla g|/k)$, $q = 1-p$ and $\left[f_x^+, f_x^-, f_y^+, f_y^-\right]$ are the gradients of positive step edges in +x, -x, +y, -y directions. For a positive boundary:

$$\begin{cases} f_x^+(x,y) = \max\{g_x(x,y),0\} \\ f_x^-(x,y) = -\min\{g_x(x,y),0\} \\ f_y^+(x,y) = \max\{g_y(x,y),0\} \\ f_y^-(x,y) = -\min\{g_y(x,y),0\} \end{cases} \quad (9)$$

and for a negative boundary:

$$\begin{cases} f_x^+(x,y) = -\min\{g_x(x,y),0\} \\ f_x^-(x,y) = \max\{g_x(x,y),0\} \\ f_y^+(x,y) = -\min\{g_y(x,y),0\} \\ f_y^-(x,y) = \max\{g_y(x,y),0\} \end{cases} \quad (10)$$

where, $(g_x, g_y) = \nabla G_\sigma \otimes I$ for gray level image I. When $p = \mu$, $q = 1$, Eq. 8 is reduced to the DDGVF. Like DDGVF, GDDGVF field is essentially a dynamic external force and cannot be directly applied to the snake model. A practical external force $F_{ext} = [F_x, F_y]$ can be derived from the GDDGVF field, which is formulated as:

$$\begin{cases} F_x = u^+ * \max\{\cos(\theta),0\} - u^- * \min\{\cos(\theta),0\} \\ F_y = v^+ * \max\{\sin(\theta),0\} - v^- * \min\{\sin(\theta),0\} \end{cases} \quad (11)$$

where, θ is the contour's normal direction at a certain snaxel. let N be the total number of snaxels, θ takes the following form:

$$\theta = \arctan\left(-\frac{x_i - x_t}{y_i - y_t}\right),\ t = \begin{cases} \left(N + (i-2)\right) \bmod N & i \neq 2 \\ N & i = 2 \end{cases},\ i = 1,2,\cdots N$$

SEGMENTATION OF THE ENDOCARDIUM AND EPICARDIUM OF THE LEFT VENTRICLE

Image preprocessing: Before running the snake models to extract the endocardium and epicardium of the LV, certain fourth-order Partial Differential Equations (PDEs) are employed for noise removal to improve image quality (You and Kaveh, 2000). Fourth-order PDEs are able to avoid the blocky effects resulted by anisotropic diffusion, while achieving the degree of noise removal and edge preservation comparable to anisotropic diffusion. Considering the following functional defined in the space of continuous images over a support of Ω:

$$E(u) = \int_\Omega f\left(|\Delta u|\right)dxdy$$

This functional minimization is a special form of the general variation problem; we can easily obtain the Euler equation which may be solved through the following gradient descent procedure:

$$\frac{\partial u}{\partial t} = -\Delta\left[f'(|\Delta u|)\frac{\Delta u}{|\Delta u|}\right] = -\Delta\left[c(|\Delta u|)\Delta u\right] \quad (12)$$

where, Δ denotes Laplacian operator and $c(|\Delta\mu|)$ is the conduct coefficient, it is supposed to be a nonnegative and decreasing function of $|\Delta\mu|$, in this study, it reads:

$$c(|\Delta u|) = \left(1 + \left(\frac{\Delta u}{h}\right)^2\right)^{-1} \quad (13)$$

When applying Eq. 12 to cardiac MR images, it can be expected that the myocardium region would be highlighted. Consequently, we are able to achieve a better edge map for GDDGVF snake model.

Initialization of snake contours: In a cardiac MR image sequence, the LV moves obviously while the surrounding structures are almost static during one cardiac cycle. This property encourages us to employ the intensity subtraction algorithm to remove stationary background structures and to localize the moving region of the LV instance. Let I (x, y, t) denote a cardiac MR image sequence, we define a new map from two consecutive frames as follows:

$$DI(x,y) = \left|I(x,y,j+1) - I(x,y,j)\right| \quad (14)$$

The nearly non-moving background pixels in two consecutive frames are excluded by the difference and the moving structures would be highlighted. Figure 1 shows a demonstration. Figure 1a and b show two consecutive frames from a cardiac MR image sequence. Figure 1c displays the difference map DI (x, y). It can be seen from this map that the moving endocardium is highlighted and this implies that the endocardium moves faster than the epicardium. Observed that the endocardium is roughly a circle, Hough transform is employed to detect this circle-like structure and the detection result can act as the initial contour for GDDGVF snake model, see the white circle centered with a cross symbol in Fig. 1d. Notably, this strategy is just used for the first frame of a sequence; the segmentation result in the previous frame can be used for the current frame.

Shape constraints: In the classical internal energy of snake model, the first derivative characterizes the continuity of the curve and the second derivative controls the smoothness. But continuity and smoothness are only local geometrical properties, if the object is partially occluded or there are weak boundaries, the snake contour would not know how to bridge such gaps in that there is no prior information about the overall shape of the object; if there are local minima caused by imperfectness of external force, the snake contour would be trapped. A solution to these issues is to incorporate the object overall shape into snake energies. Observed that the endocardium of the LV is roughly a circle, we previously proposed a circle-shape constraint for tasks on hand, which is formulated as (Wang and Jia, 2006):

$$E_{circle} = \frac{\lambda}{2}\int \left(R_x - \bar{R}\cos(2\pi s)\right)^2 + \left(R_y - \bar{R}\sin(2\pi s)\right)^2 ds \quad (15)$$

Where:

$$R_x(s) = x(s) - \int_0^1 x(r)dr$$

$$R_y(s) = y(s) - \int_0^1 y(r)dr$$

$$\bar{R} = \int_0^1 \sqrt{R_x^2(s) + R_y^2(s)}ds$$

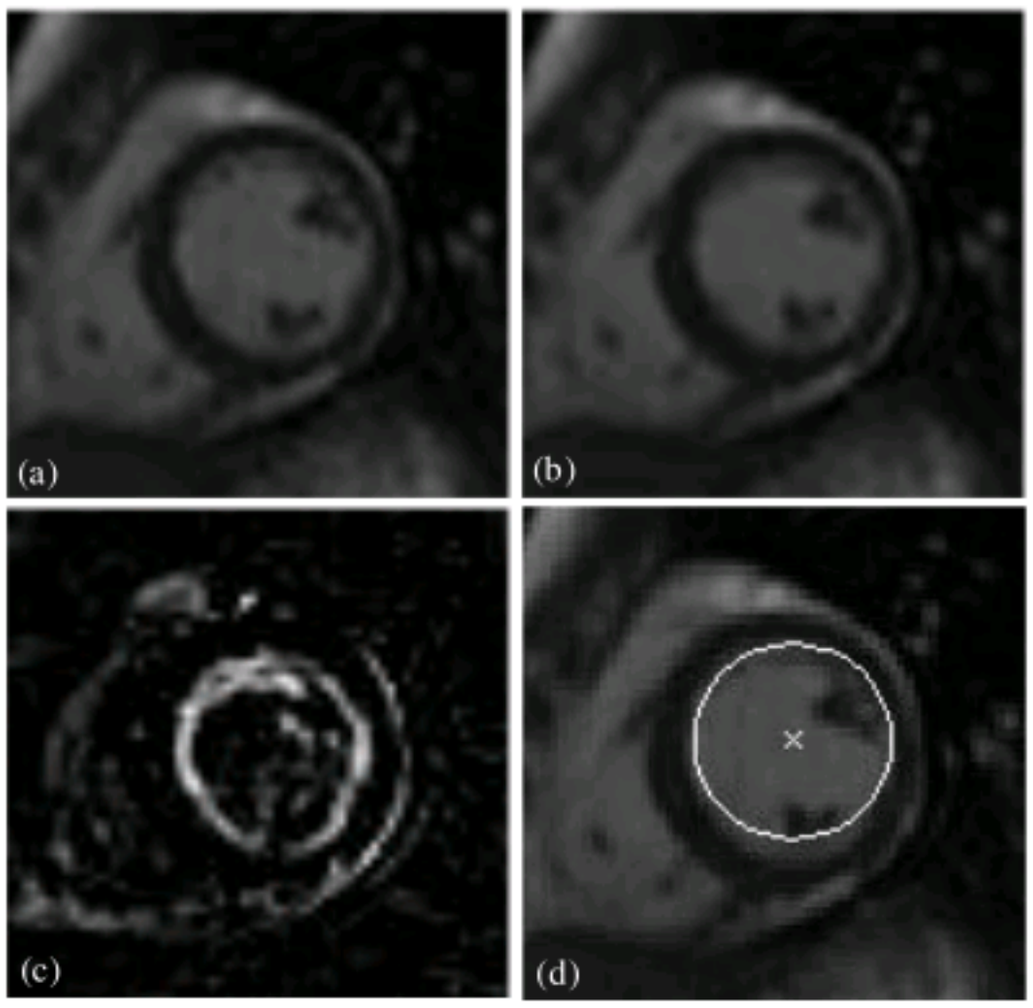

Fig. 1: (a, b) Two consecutive frames in a cardiac MR image sequence, (c) intensity difference map and (d) detection result by applying Hough transform to (c)

This constraint tries to make the snake contour a circle during evolution. In fact, E_{circle} measures the deviation of the snake contour from a circle of radius $\overline{R}$, which can be considered as the mean shape of the evolving snake contour. If there is no external force, the snake contour would just be a circle. This constraint will incorporate energy (2) to regularize the snake contour.

In Fig. 2, we illustrate segmentation of the endocardium and epicardium using the circle-shape energy to conquer the papillary muscle and artifacts. There are four panels and for each panel, the left one is the result without shape constraint and the right one is with shape constraint. Figure 2a and b show segmentation results of the endocardium; it can be seen

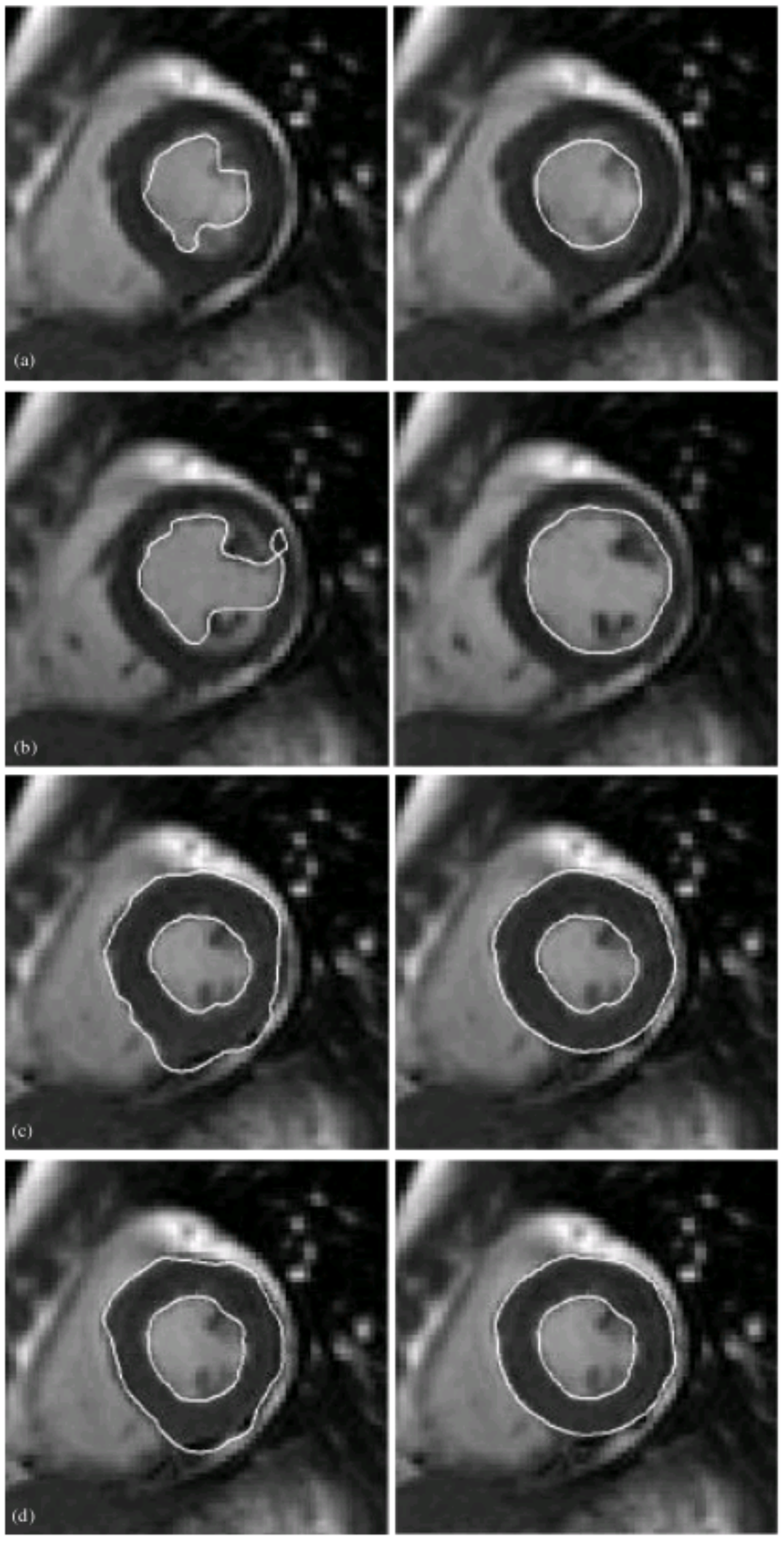

Fig. 2: Effectiveness of shape constraints on segmentation of the (a, b) endocardium and (c, d) epicardium

that the papillary muscle and artifacts are well excluded by using the circle-shape energy. Figure 2c and d are shown segmentation of the epicardium, the snake contour would leak out from weak boundaries (left), but when the shape energy is incorporated, the snake contour behaves satisfactorily (right).

Segmentation of the endocardium and epicardium: Algorithm summary: In summary, there are eight steps in the flowchart of the algorithm for segmentation of the endo- and epicardium as follows:

- Remove noise in images using Eq. 12-13.
- Calculate $f_x^+, f_x^-, f_y^+, f_y^-$ for the endocardium boundaries of the image using Eq. 9.
- Calculate GDDGVF field $u^+(x, y)$, $u^-(x, y)$, $v^+(x, y)$, $v^-(x, y)$ and the external force using Eq. 8 and 11.
- Initialize the snake contour for endocardium using Eq. 14 for the first frame in a sequence and using the segmentation result in the previous frame for current frame.
- Extract the endocardium using snake model with shape constraint in Eq. 15 and GDDGVF external force until convergence.
- Calculate $f_x^+, f_x^-, f_y^+, f_y^-$ for the epicardium boundaries of the image using Eq. 10.
- Calculate GDDGVF field $u^+(x, y)$, $u^-(x, y)$, $v^+(x, y)$, $v^-(x, y)$ and the external force using Eq. 8 and 11.
- Extract the epicardium by taking the endocardium contour as initialization and using snake model with strategies as for endocardium.

EXPERIMENTAL RESULTS AND ANALYSIS

Here, we will demonstrate the effectiveness of the proposed strategies for cardiac MR image segmentation and the performance of the GVF, DDGVF and GDDGVF snakes are compared. We use $h = 0.5$ and iteration number 20 for 4th-order PDEs based noise removal, $\alpha = 1$, $\beta = 1$, time step $\tau = 0.5$, $\lambda = 1.2$, for snake models and all the experiments are conducted on a PC with Pentium D 3.4-GHz CPU, 1-GB RAM, MATLAB 2007a and Windows XP Professional. The *in vivo* heart images used in this study are acquired on a 1.5T Siemens clinical MR system using breath-hold techniques, with the following parameters: image dimension 192×156, pixel size 1.82×1.82 mm^2, slice thickness 8 mm, repetition time 29.16 msec, echo time 1.08 msec, Flip angle 60, field of view 320, 21 phases per cycle.

Comparison of GVF snake, DDGVF snake and GDDGVF snake: The aim of this experiment is to compare the performance of the GVF, DDGVF and GDDGVF snakes for extraction of endocardium and epicardium of the left ventricle and to verify that the GDDGVF snake outperforms the other two ones. The GVF, DDGVF and GDDGVF are calculated using 250 iterations and $\mu = 0.05$ for GVF and DDGVF and $k = 0.05$ for GDDGVF. The performance of GVF, DDGVF and GDDGVF snakes when applied to cardiac images is shown in Fig. 3. As shown in Fig. 3a, the GVF snake can't locate the endocardium at all using the given initialization due to the critical point problem lurked in GVF snake (Wang and Jia, 2007) that is, the initial contour should enclose the inner critical points and exclude the outer ones, otherwise, the convergent results would be far from expected. As shown in Fig. 3d, incorporating the strategies proposed in (Wang and Jia, 2006) the GVF snake can fairly accurately locate the epicardium, but the fat surrounding the epicardium confused the snake contour, this can be clearly seen in the zoomed in version in Fig. 4a. It can be seen from Fig. 3b and e that the DDGVF snake can't accurately locate the endocardium and epicardium because the negative and positive boundaries stemming from papillary muscles disturbed the snake contour and the snake contour is trapped.

Figure 3c and f show the results of GDDGVF snake, because the GDDGVF snake takes the edge information into account, it conquered the spurious edges resulted by the papillary muscles; the GDDGVF snake also possesses the desired properties of distinguishing the positive and negative boundaries of DDGVF snake, it discerned the fat surrounding the epicardium and accurately located the epicardium, see the close-up of Fig. 3f in 4b.

Segmentation results: The proposed method has been applied to a set of *in vivo* dataset to test its performance. In our dataset, there are 7 image slices spanning the whole left ventricle and there are 21 images acquired throughout one cardiac cycle on each slice. Figure 5 shows the segmentation results of the images from one slice with papillary muscles. By taking the manual collections as ground truth, the results by the proposed methods are evaluated using Mean Absolute Distance (MAD). Let $S = \{s_1, ..., s_n\}$ be the snake contour and $M = \{m_1,..., m_k\}$ be the manually delineated contour, the MAD between two contours S and Mis defined as:

$$mad(S,M) = 0.5\left(\frac{1}{n}\sum_{i=1}^{n} d(s_i,M) + \frac{1}{k}\sum_{j=1}^{k} d(m_j,S)\right) \qquad (16)$$

where, $d(s_i,M) = \min_j \|s_i - m_j\|$. For endocardium, among the 147 MADs, the Mean MAD is 0.73 pixels; but

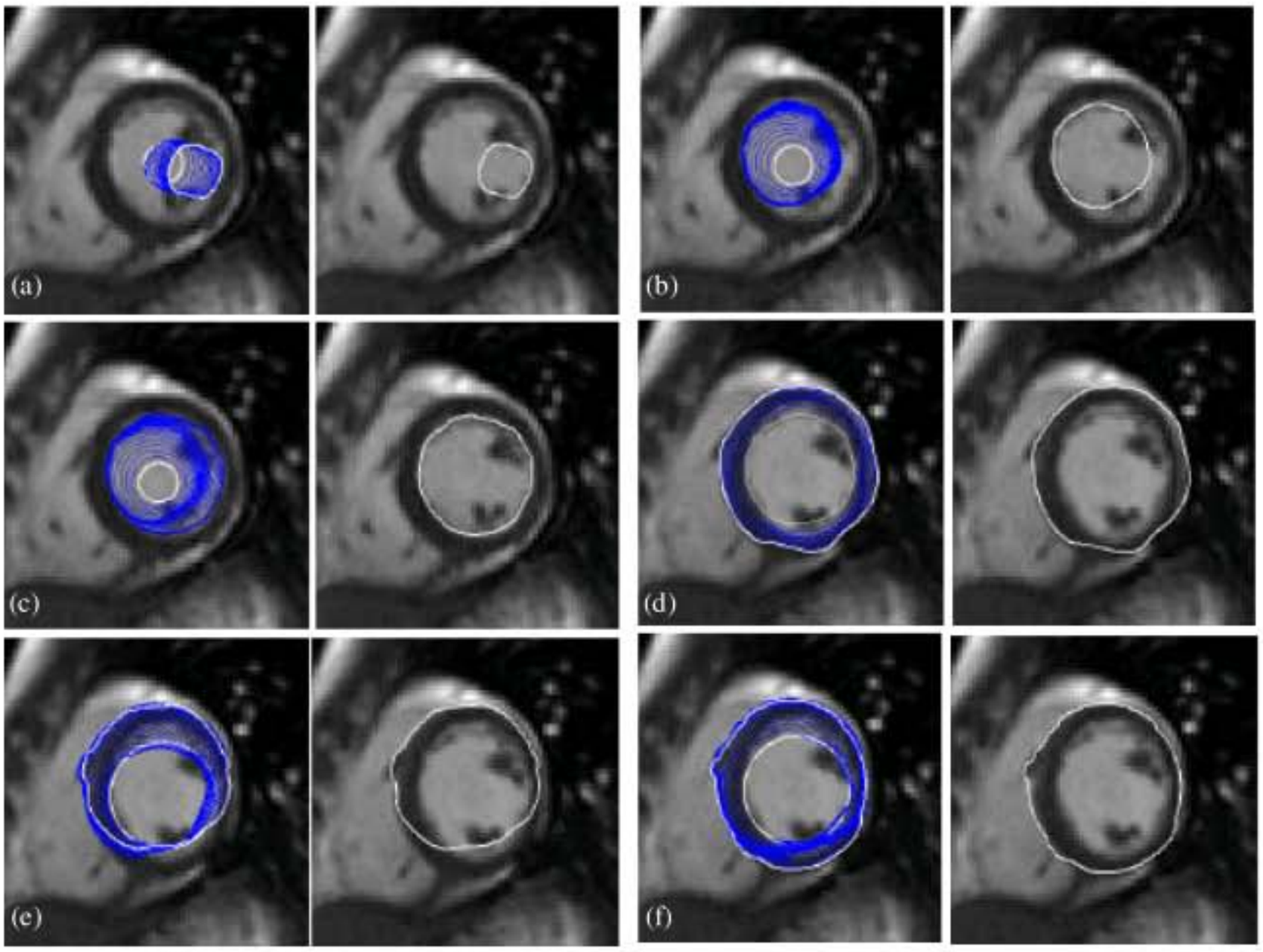

Fig. 3: (a-f) Performance of GVF, DDGVF and GDDGVF snakes. Segmentation of the endocardium (upper row) and the epicardium (lower row) with the same initial contours using three different external forces. First column: results of boundary detection using GVF snakes. Second column: results of boundary detection using DDGVF snakes. Third column: results of boundary detection using GDDGVF snake. In each panel, the left one is the image with the initial contour and the successive contours overlaid and the right one is that with the convergent contour

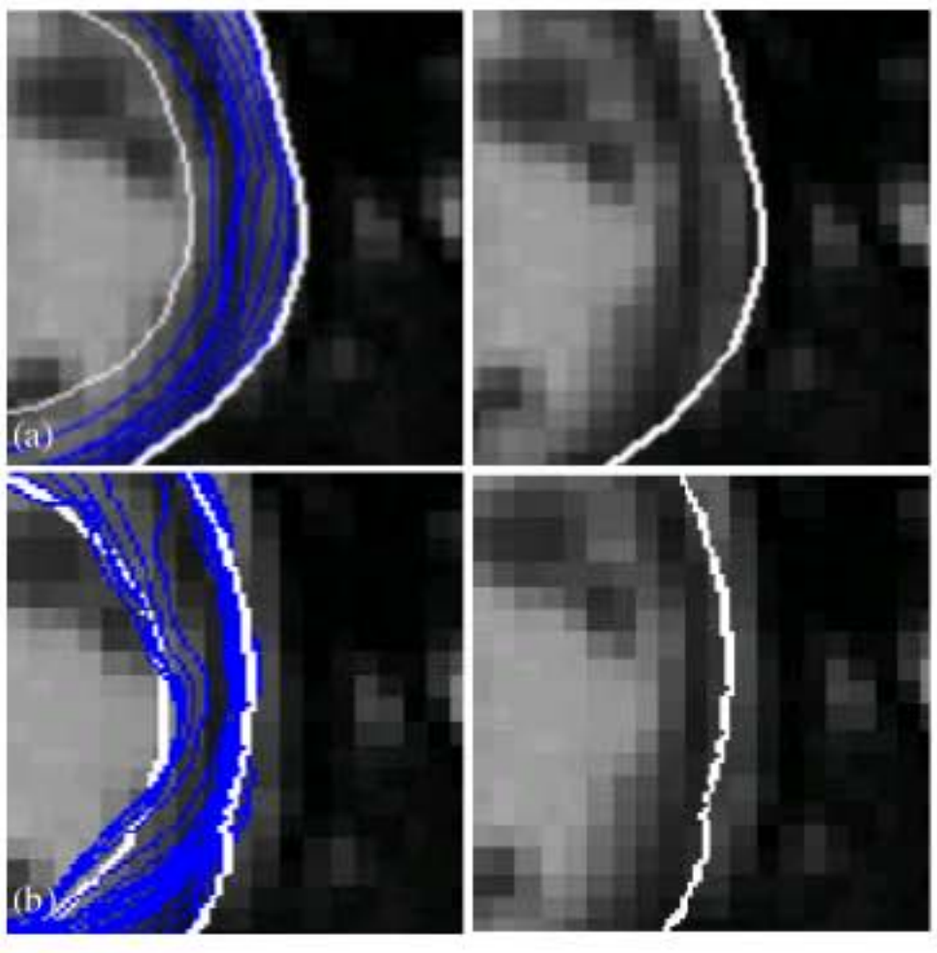

Fig. 4: Close-up of Fig. 3d and f; (a) Close-up of Fig. 3d and (b) close-up of Fig. 3f

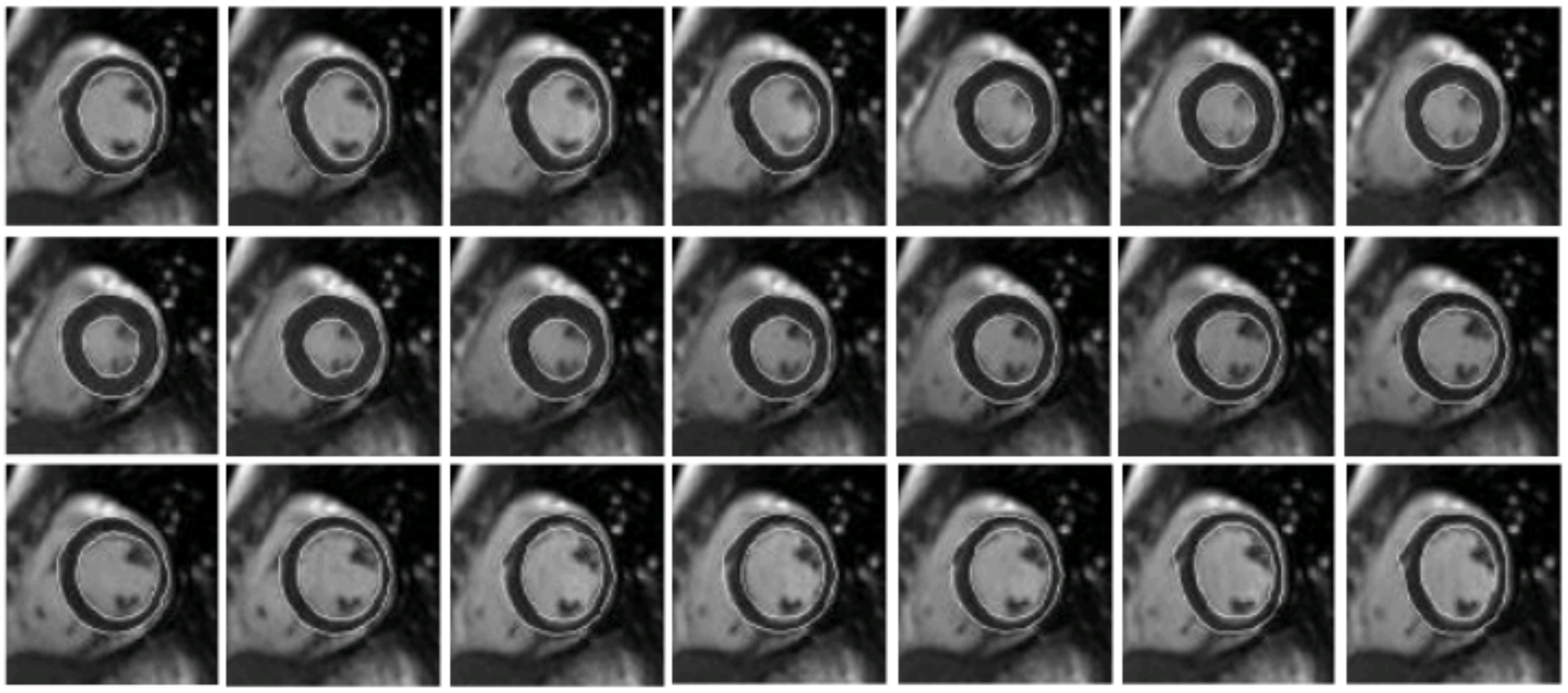

Fig. 5: Segmentation of the endocardium and epicardium of the left ventricle using GDDGVF snakes

for epicardium, the mean MAD is 0.66 pixels and the average MAD is 0.7 pixels. This result is much better than that proposed by Wang and Jia (2006), especially for the epicardium, where the MAD is 2.06 pixels.

CONCLUSION

The scope of this contribution is to introduce a novel approach for segmentation of the endocardium and epicardium of the left ventricle in MR images. The proposed method is based on GVF snake model by introducing two effective strategies, firstly, the GDDGVF external force is introduced, this new external force can distinguish the positive and negative boundaries as DDGVF and overcome the spurious edges raised by artifacts by taking the edge information into account; secondly, based on the observation that the left ventricle is roughly a circle, a circle shape constraint is incorporated into the snake model, this novel constraint can push the snake contour across the artifacts and papillary muscles when applied to endocardium and keep the snake contour away from being trapped and leaking out when applied to epicardium. The proposed strategies have been applied to a set of *in vivo* human heart data and satisfactory segmentation results were achieved.

ACKNOWLEDGMENT

This study was supported by the National Natural Science Foundation of China under grants No. 60602050 and No. 60805004.

REFERENCES

Bosch, H.G., S.C. Mitchell, B.P.F. Lelieveldt, F. Nijland, O. Kamp, M. Sonka and H.C. Reiber Johan, 2001. Active appearance-motion models for fully automated endocardial contour detection in time sequences of echocardiograms. Proceedings of the 15th International Congress and Exhibition on Computer Assisted Radiology and Surgery, June 27-30, Elsevier Science BV., Berlin, Germany, pp: 941-947.

Chen, W.F., S.J. Zhou and B. Liang, 2004. LV contour tracking in MRI sequences based on the generalized fuzzy GVF. Proceedings of 2004 International Conference on Image Processing (ICIP 2004), Oct. 24-27, IEEE, Singapore, pp: 373-376.

Cheng, J. and F. Say Wei, 2006. Dynamic directional gradient vector flow for snakes. IEEE Trans. Image Process., 15: 1563-1571.

Folkesson, J., E. Samset, R.Y. Kwong and C.F. Westin, 2008. Unifying statistical classification and geodesic active regions for segmentation of cardiac MRI. IEEE Trans. Inform. Technol. Biomed., 12: 328-334.

Fujino, T., S. Ono, K. Murata, T. Nobuaki and T. Takashi *et al*., 2001. New method of on-line quantification of regional wall motion with automated segmental motion analysis. J. Am. Soc. Echocardiogr, 14: 892-901.

Hautvast, G., S. Lobregt, M. Breeuwer and F. Gerritsen, 2006. Automatic contour propagation in cine cardiac magnetic resonance images. IEEE Trans. Med. Imaging, 25: 1472-1482.

Kass, M., A. Witkin and D. Terzopoulos, 1988. Snakes: Active contour models. Int. J. Comput. Vision, 1: 321-331.

Lalande, A. and M. Jaulent, 1996. A fuzzy automaton to detect and quantify artery lesions from arteriograms. Proceedings of the 6th International Conference on Information Processing and Management of Uncertainty in Knowledge-Based Systems, IPMU'96, Granada, Spain, pp: 1481-1487.

Makowski, P., T.S. Sorensen, S.V. Therkildsen, M. Andrzej and S.J. Hans, 2002. Two-phase active contour method for semiautomatic segmentation of the heart and blood vessels from MRI images for 3D visualization medical. Comput. Med. Imaging Graph., 26: 9-17.

Osher, S. and J.A. Sethian, 1988. Fronts propagating with curvature dependent speed: Algorithms based on hamilton-jacobi formulation. J. Comput. Phys., 79: 12-49.

Paragios, N., 2003. A level set approach for shape drive segmentation and tracking of the left ventricle. IEEE Trans. Med. Imaging, 22: 773-776.

Pluempitiwiriyawej, C., J.M.F. Moura, W. Yi-Jen Lin and H. Chien, 2005. STACS: New active contour scheme for cardiac mr image segmentation. IEEE Trans. Med. Imaging, 24: 593-603.

Ranganath, S., 1995. Contour extraction from cardiac MRI studies using snakes. IEEE Trans. Med., 14: 328-338.

Siddiqi, K., Y.B. Lauziere, A. Tannenbaum and S.W. Zucker, 1998. Area and length minimizing flows for shape segmentation. IEEE Trans. Image Process., 7: 433-443.

Wang, Y. and Y. Jia, 2006. Segmentation of the left ventricles from MR images via snake models incorporating shape similarities. Proceedings of 2006 International Conference on Image Processing (ICIP 2004), Oct. 8-11, IEEE, Atlanta, GA, USA, pp: 213-216.

Wang, Y.Q., J. Liang and Y. Jia, 2007. On the critical point of gradient vector flow snake. Proceedings of 8th Asian Conference on Computer Vision (ACCV 2007), Nov. 18-22, LNCS., Tokyo, Japan, pp: 754-763.

Xu, C. and J.L. Prince, 1998. Generalized gradient vector flow external force for active contours. Signal Process., 7: 131-139.

Xu, C.Y. and J.L. Prince, 1998. Snakes, shapes and gradient vector flow. IEEE Trans. Image Process., 7: 359-369.

You, Y.L. and M. Kaveh, 2000. Fourth-order partial differential equations for noise removal. IEEE Trans. Image Process., 9: 1723-1730.